Powder Technology 356 (2019) 39–49

Contents lists available at ScienceDirect

Powder Technology

journal homepage: www.elsevier.com/locate/powtec

Effect of SiO_2 nanoparticles on the heat transfer characteristics of refrigerant and tribological behaviour of lubricant

S.S. Sanukrishna [a,b,c,*], Muhammed Shafi [b], Maneesh Murukan [b], M. Jose Prakash [b]

[a] University of Kerala, Thiruvananthapuram, Kerala, India
[b] Department of Mechanical Engineering, T.K.M. College of Engineering, Kollam, Kerala 691005, India
[c] Sree Chitra Thirunal College of Engineering, Thiruvananthapuram, Kerala 695018, India

ARTICLE INFO

Article history:
Received 11 March 2019
Received in revised form 20 July 2019
Accepted 23 July 2019
Available online 24 July 2019

Keywords:
Nanolubricant
Heat transfer coefficient
Enhancement factor
Coefficient of friction
Wear scar

ABSTRACT

Scientists and researchers are enthusiastically utilizing novel technologies that can substantially reduce energy consumption in diverse thermal systems. The foremost aim of the present investigation is to exploit the potential of nanoparticles on the enhancement of heat transfer characteristics of refrigerant and tribological capabilities of lubricant. Experimental investigations on the forced convection heat transfer characteristics of R134a/SiO_2 nanorefrigerant (R134a + SiO_2-polyalkylene glycol nanolubricant) are carried out. The effect of particle concentration, heat flux, mass flux, and vapour quality are investigated. The friction reduction and anti-wear properties of the nanolubricant are evaluated using four-ball tribo-tester. The results reveal that the presence of nanoparticles in the refrigerant significantly enhances the heat transfer coefficient of refrigerant and the tribological behaviour of lubricant. The maximum increase in heat transfer coefficient is 163.2% corresponding to a particle concentration of 0.4%. The presence of nanoparticles in refrigerant results in a marginal increase in pressure drop. However, the penalty in pressure drop is insignificant compared to the enhancement in heat transfer. Excellent friction reduction and anti-wear performance are also manifested by the nanolubricant. The maximum reduction in the friction coefficient is 37.76% and that of wear scar diameter is 40.83%. Considering the heat transfer and tribological characteristics, the optimum value of the particle volume fraction is 0.4%. SiO_2-PAG nanolubricant can be considered as a potential energy-saving alternative to refrigerant compressor oils.

1. Introduction

The enhancement of thermal properties of fluids by the dispersion and stabilization of solid particles was established by Maxwell [1] more than a century ago. The concept of nanofluid as the next generation heat transfer media was first introduced by Choi et al. [2]. Nanofluids are engineered colloidal suspensions of nanoparticles in base fluids. Nanofluids have unique features which are quite different from those of conventional solid-liquid mixtures in which millimeter and/or micrometer-sized particles are added. Micro/mm-sized particles settle rapidly, clog flow channels, erode pipelines and cause severe pressure drops. All these shortcomings prohibit the application of conventional solid-liquid mixtures. Stably suspended ultrafine nanoparticles dramatically improve the thermophysical and heat transfer characteristics of the mixture and improve its capability of energy exchange.

Nanorefrigerants are nanofluids in which nanoparticles are suspended in the refrigerant host fluid. The nanorefrigerants are of two kinds, refrigerant-based and nanolubricant based. In the former nanoparticles are directly dispersed into refrigerants, while in the latter lubricant appended with nanoparticles is ultimately circulated along with refrigerants [3]. Recently scientists use nanoparticles in refrigerants to improve the energy efficiency and overall performance of HVAC systems. In refrigeration systems, when the refrigerant is circulated through the compressor it carries traces of nanolubricant so that the other parts of the system will have nanolubricant -refrigerant mixture. Addition of nanoparticles in refrigerants results in remarkable improvement in thermophysical, and heat transfer capabilities which in turn enhances the efficiency and reliability [4–6].

The boiling behavioural study of refrigerants appended with nanoparticles has great importance. The two-phase flow boiling phenomena is complex in nature; it may become more complex in the presence of nanoparticles. The nanofluid research community published limited experimental studies concern to boiling phenomena in nanorefrigerants. Most of the studies are pertaining to pool boiling phenomena and are conflicting in many ways as well. Liu and Yang [7] examined the effect of Au nano-additive on the nucleate pool boiling characteristics of R-141b. The results revealed the pool boiling heat transfer improving

Abbreviations: COP, coefficient of performance; EF, enhancement factor; HTC, heat transfer coefficient; HVAC, Heating, ventilation and Air conditioning; PAG, polyalkylene glycol; TEM, transmission electron microscope; SEM, scanning electron microscope; Uv-vis, Ultraviolet visible.

* Corresponding author at: Sree Chitra Thirunal College of Engineering, Thiruvananthapuram, Kerala 695018, India.

https://doi.org/10.1016/j.powtec.2019.07.083
0032-5910/

Nomenclature

Cp	specific heat [kJ/kg K]
h	heat transfer coefficient [W/m^2 K]
H	enthalpy [kJ /kg]
k	thermal conductivity [W /m K]
m	mass of nanoparticles [g]
M	mass flow rate [kg/ s]
Pr	Prandtl number
Re	Reynolds number
T	temperature [°C]
x	vapour quality

Greek symbols

φ	volume fraction [%]
μ	dynamic viscosity [cP]
ρ	density [kg/ m]

Subscripts

bub	bubble point
bf	base fluid
f	fluid
g	gas
eff	effective
i	inside
in	inlet
l	liquid
np	nanoparticle
o	outside
out	outlet
p	particle
pre	pre-heater
sat	saturation
test	test section
w	wall
fg	liquid gas mixture
r,o	refrigerant oil mixture
r,n,o	refrigerant nano-oil mixture
tp	two-phase

potential of Au particles. Enhancement in nucleate pool boiling HTC of nanorefrigerant is reported by Park and Jung [8] also. The experimental evaluation of two-phase flow boiling heat transfer characteristics of nanorefrigerants is scarce. Interestingly, both enhancement and detriment effects in flow boiling heat transfer with the addition of nanoparticles are reported in the literature. Peng et al. [9] reported the influence of CuO nanoparticles in R113 refrigerant flow boiling inside a horizontal smooth tube. According to their studies, the heat transfer coefficient of refrigerant mixed with nanoparticles was higher than that of pure refrigerant. Henderson et al. [10] quantified the influence SiO_2 nanoparticles on flow boiling of R134a and show that direct dispersion of SiO_2 nanoparticles in R134a results in the decrease of heat transfer coefficient. Sun and Yang [11] portrayed the flow boiling characteristics of four types R141based nanorefrigerants with different nanoparticles and concluded that at constant mass velocities, the concentration of nanoparticles is the major factor which influences the heat transfer coefficient. Akhavan-Behabadi et al. [12] researched the influence of CuO nanoparticles on flow boiling of R600a/oil mixture and an improvement in the flow boiling heat transfer coefficient is reported. The phase change heat transfer is a key area of research as far as nanorefrigerants are concerned. Controversies are still subsisting and the scientific community has not arrived at an ample conclusion. Contradictory results should not disparage researchers but increase the enthusiasm and encourage them to concentrate on the key research frontline.

Addition of chemical compounds, commonly known as additives, has been a well-known practice to enhance the tribological characteristics of lubricants [13]. Fine solid metal particles have also been employed as anti-friction and anti-wear additives to oils for enhancing their thermophysical and tribological properties [33,34]. According to the investigations [14–17] that have been conducted, the presence of nanoparticles in oils may enhance their lubricating properties, this would, in turn, result in an increase in the durability of the components. Castillo and Spikes [18] investigated the lubricating behavior of simple colloidal systems consists of silver and carbon black particles and mineral oil. They studied the effect of nanoparticles on the contact surfaces. The results exposed the formation of a tribo-film at lower speeds when the lubricant film thickness is less than the particle diameter and its disappearance at higher speeds. The silver-based nanolubricant reduces friction and wear in the thin film regime, but the carbon black colloid shows a negligible beneficial effect. The lubrication mechanism of nanoparticles is found to be complex since there are large numbers of nanoparticles and each of them may work in different ways in diverse applications [19].

Even though few studies are available in the literature regarding the capabilities of nanoparticles as an additive to lubricants, the studies with refrigerant compressor oil based nanolubricants are scarce. The HVAC industry has been working actively to improve the efficiency of various thermal systems. Improved efficiency could eventually result in reduced energy consumption, reduced global warming and other favourable influences on sustainability. This will generate a necessity to evaluate the heat transfer performance of nanorefrigerants as well as the tribological potentials of nanolubricants.

The present study focuses on the experimental investigations on the two-phase flow boiling heat transfer characteristics of R134a refrigerant appended with SiO_2-PAG nanolubricant in a horizontal smooth tube at various particle concentrations, heat fluxes, mass fluxes, and vapour qualities. Furthermore, tribological characterization of polyalkylene glycol oil dispersed with SiO_2 nanoparticles at different particle concentrations is conducted to elucidate the friction reduction and anti-wear capabilities. The result obtained from this study will be useful in developing energy-efficient and compact refrigeration systems.

2. Experimental method

2.1. Materials and characterization

SiO_2 nanoparticles,(purity: 99.8%) spherical in shape supplied by Sigma Aldrich Limited, USA is used in the present study. The particle size is in the range the 10-20 nm, molecular weight is 60.08 g/mol, the boiling point is 2230 °C and density is 2.6 g /cm^3 The commercially available, fully synthetic, oil, based on Polyalkylene Glycol (PAG) with a nominal liquid dynamic viscosity of 30–40 cP at 40 °C, is used as the base fluid. Scanning Electron Microscopy (SEM) and Transmission electron Microscopy (TEM) are employed for the morphological characterization of SiO_2 nanoparticles and nanolubricant respectively. Fig. 1(a) shows the SEM image of dry SiO_2 nanoparticles, which reveals the distribution and shape of the nanoparticles. It can be seen that the particles are in the form of agglomerates. These agglomerates have to be broken during the preparation of nanolubricant to produce a stable suspension. It can be accomplished through magnetic agitation and subsequent ultra-sonication.

2.2. Preparation of nanolubricant

Preparation of nanolubricant is the primary step in the experimental studies. Nanofluids are not mere solid to fluid suspensions. In order to achieve even, stable and durable suspension with a negligible aggregation of particles, special procedures are necessary. Nanolubricant samples are prepared by the two-step method and no surfactants are added. Nanolubricants are prepared at four different particle

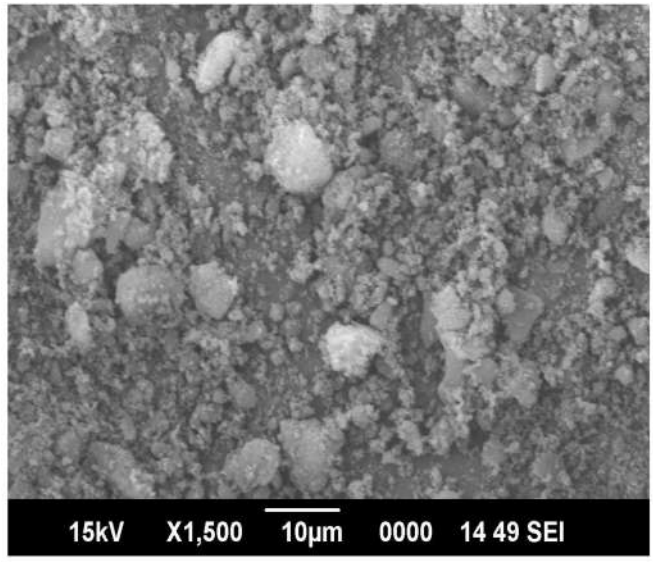

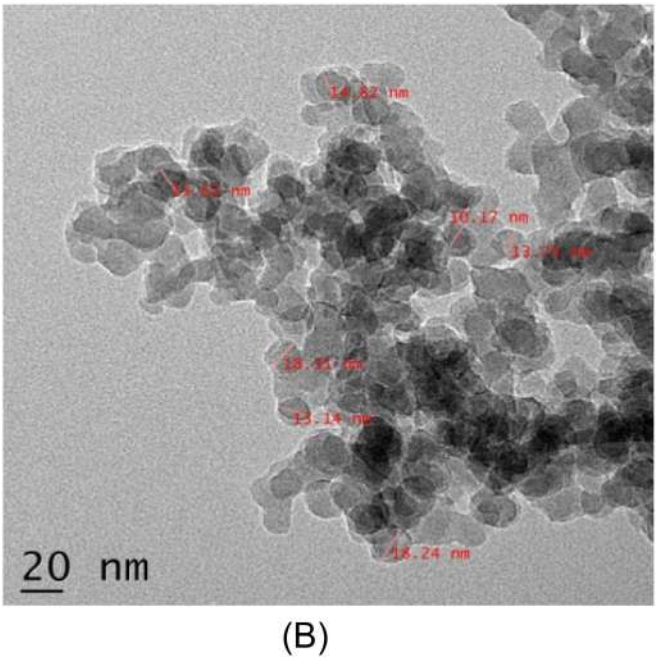

Fig. 1. (a) SEM image of dry SiO_2 nanoparticles (b) TEM image of SiO_2 suspension.

concentrations (0.1, 0.4, 0.6 and 0.8vol. %). The required mass of nanoparticles corresponding to the volume fractions is calculated (Eq. (1)) and weighed using a high precision electronic balance.

$$\Phi = \frac{\left(m/\rho\right)_{SiO_2}}{\left(m/\rho\right)_{SiO_2} + \left(m/\rho\right)_{PAG}} \quad (1)$$

The preliminary mixing process of samples is carried out using the magnetic stirrer for 1 h and then agitated using ultrasonic agitator (BRANSON-3800) at a frequency of 40 kHz intermittently for 6 h with sufficient cool-off period in a controlled atmosphere (25-30 °C) to homogenize the samples. No evidence of sedimentation or coagulation was noticed after 120 h of preparation.

Fig. 1(b) shows the TEM image of the SiO_2 suspension. According to the TEM image, the nanoparticles have almost similar morphological characteristics such as physical appearance, shape, and size in the dispersion and are well distributed also. The average size of nanoparticle was found to be 14.26 nm.

2.3. Stability studies

Dispersion stability of the nanolubricant is conducted by spectral absorbency analysis with UV–vis spectroscopy, which is one of the most effective techniques to study the stability of nanofluids. The dispersion stability was evaluated at room temperature by measuring the absorbance after 1st day and 5th days of preparation. The principle of working of Uv-vis spectroscopy is the Beer-Lambert law, which states that the absorbance is directly proportional to the concentration of the species in the colloid, absorptivity of the species and the path length [35]. Fig. 2 shows the UV–vis spectra of the nanolubricant. The SiO_2 particle concentration considered for the stability study is 0.6 vol%. The peak absorbance obtained for the SiO_2-PAG sample after the first day and fifth day of preparation is 6.0 at a wavelength of 311 nm. This is an indication of the presence of a higher population of nanoparticles in the nanolubricant to interact with the light, which shows the stability.

2.4. Flow boiling heat transfer studies

Flow boiling heat transfer studies on pure refrigerant and nanorefrigerants are conducted to ascertain the effect of nanoparticles on the flow boiling heat transfer coefficient of the refrigerant R 134a.

2.4.1. Experimental test-rig

Experimental set up to conduct forced convective heat transfer studies is designed and fabricated in-house. The experiments are designed according to ASTM D7863–17 standard. It is an international standard developed in accordance with internationally recognized principles on standardization and is a guide for the evaluation of convective heat transfer coefficient of fluids in circular conduits. It covers the information regarding the selection of methods for the evaluation of heating and cooling performance of heat transfer fluids where forced convection is the mode of heat transfer. Fig. 3 shows the schematic diagram of the experimental setup.

The experimental apparatus includes a gear pump, flow meter, preheater, test section, by-pass circuit, and a condenser. The preheater is installed in the upstream of the test section to obtain the desired vapour quality at the inlet of the test section. The test section is a smooth horizontal copper tube with an outside diameter of 12.7 mm, thickness 0.7 mm and an effective length of 830 mm. A gear pump with a maximum capacity of 1500 kPa is used to circulate the refrigerant in the

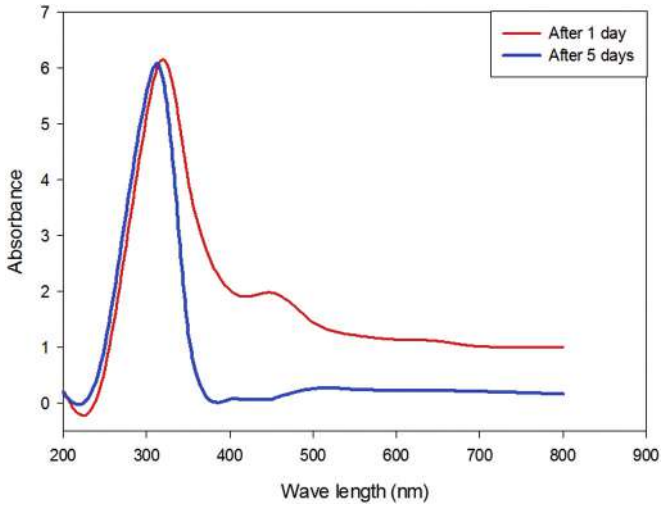

Fig. 2. UV–vis spectra of the SiO_2-PAG nanolubricant (0.6 vol%).

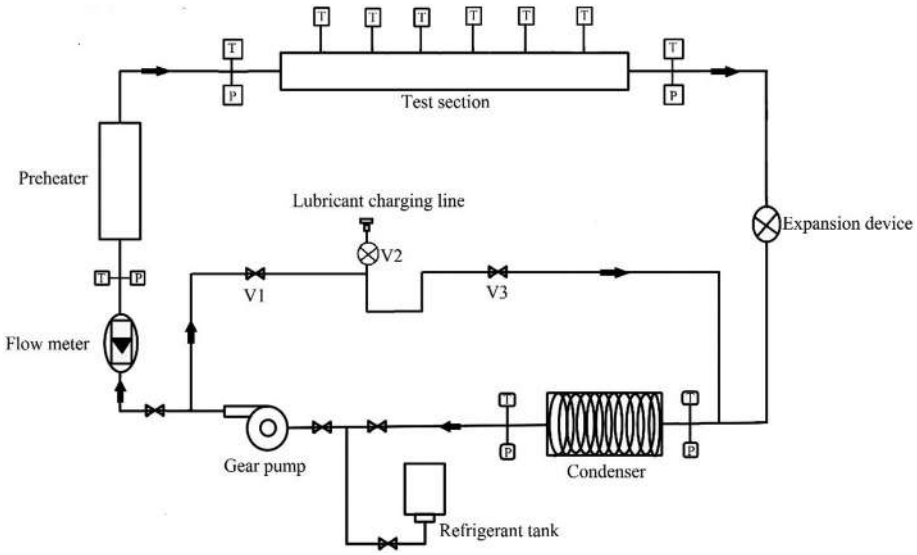

Fig. 3. Schematic diagram of the experimental setup.

cycle and to compensate for pressure drop. A condenser coupled with a constant temperature circulator is used in the experimental set up to condense the refrigerant from the test section. The temperature of the condensing medium is kept well below the saturation temperature of the refrigerant corresponding to the pressure to assure saturated liquid at the inlet of the pump. A flow meter with an accuracy of ±1.75% of full scale is used to measure the refrigerant mass flow. Two tape heaters of 25 mm width and 1000 mm length are wrapped uniformly around the test section and pre-heating sections and which are used as the heat input source. The test section and pre-heating sections are thermally insulated by glass wool pads and asbestos rope to reduce the heat loss to the surroundings. Thermocouples are fixed on the surface of the test section using thermal epoxy. The outside tube wall temperature is measured by T-type thermocouples (with an accuracy of ±0.5 °C) fixed at 6 positions along the test section. The heat energy supplied to the test section and pre-heating sections is assumed to be uniform. The pressures at salient points are measured by pressure transducers with an accuracy of 1 kPa. The input power of each heater is controlled by a dimmerstat. The refrigerant mass flow is carefully controlled by the needle valve and the bye- pass circuit, which permits fine control over the mass flow. Nanolubricant charge line is incorporated with the bye-pass circuit. The experimental set up is tested thoroughly for any leaks before conducting experimentations. Before charging the circuit with refrigerant, the required amount of nanolubricant is injected into the oil charge port and closed with end plug. The mass fraction of lubricant is limited to 2% because mass fraction beyond 2% results in a significant deterioration in heat transfer [23]. A known quantity (350 g) of refrigerant R134a is then charged into the circuit through the charging line and the pump runs for 1 h to homogenize the lubricant and refrigerant. During each experimental test run, five sets of data were taken at intervals of 10 min each after the system reached a steady-state condition.

The temperature and pressure at the inlet of the pre-heating section are continuously monitored and based on this it is assured that the fluid is always saturated at the inlet of the pre-heating section. The enthalpies at the preheating section and test section are evaluated using measured temperatures and pressures. The heat transfer coefficient is calculated based on the equations for pure refrigerant since the presence of oil (2%) is not significant enough to affect the saturation temperature of the refrigerant and thermodynamic cycle of the system beyond the uncertainty. Baseline tests are conducted with pure refrigerant and heat transfer coefficient is compared with that obtained from correlation for R134a [20]. The experiments are then conducted with R134a/pure lubricant and R134a/SiO_2 nanolubricant at different volume fractions (0.1, 0.4 and 0.8 vol%) to observe the effect of the addition of nanoparticles on the flow boiling heat transfer characteristics of refrigerant. The flow boiling heat transfer test rig is cleaned with acetone after each experiment with nanolubricant and the baseline tests with pure refrigerant are repeated to confirm whether any deviation in test results due to the entrapment of nanoparticles inside the test rig. No significant changes are observed in the repeated tests, it indicates that there is no permanent modification inside the test rig due to the presence of nanoparticles. The experimental conditions are shown in Table 1

2.5. Data reduction

2.5.1. Heat transfer coefficient

The boiling point of the refrigerant-oil mixture is slightly higher than that of pure refrigerant. Thome [21] proposed that the correct thermodynamic manner to calculate the heat transfer coefficient is using the bubble point temperature, T_{bub} instead of T_{sat}, and also reported that the difference between T_{sat} and T_{bub} becomes significant only when the vapour quality is higher than 80%. The bubble point temperature of R134a-PAG oil with an oil concentration of 2% is calculated using the empirical correlation [22,23] and no difference between the saturated temperature and bubble point temperature is observed. Therefore the local flow boiling heat transfer coefficient is calculated according to Eq. (2).

$$h = \frac{q}{T_{w,i} - T_{sat}} \tag{2}$$

where, h is the heat average transfer coefficient, W/m^{2}K, q is the heat flux in W/m^2, $T_{w,i}$ is the inside tube wall temperature in °C, T_{sat} is the saturation temperature of the refrigerant, which is determined by the vapour pressure curve and the measured pressure. The inside tube wall temperature is calculated by the heat conduction equation based on

Table 1
Experimental conditions.

Parameters	Range
Refrigerant	R134a
Lubricant oil	Poly alkylene glycol
Mass fraction of oil (%)	2
Nanoparticle	SiO_2
Nanoparticle volume fraction (%)	0.1,0.4 and 0.8
Mass flux (kg/m^{2}s)	34 and 47
Vapour quality	0 to 0.5
Heat flux (kW/ m^2)	0.45 to 5.0
Pressure(kPa)	450–800

the measured outside tube wall temperature,

$$\mathrm{Tw,i} = \mathrm{Tw,o}\,\frac{Q_{test}\ \ln(d_0/d_i)}{2\pi k_c \mathrm{L}} \tag{3}$$

where, Q_{test} is the heat applied to the test section in W, d_o and d_i are the outside and inside diameter of the test section respectively in m. k_c is the thermal conductivity of the copper tube in W/m K, L is the effective heating length of the test section in *m* and $T_{w,o}$ is the outside wall temperature of the test section, which is equal to the arithmetic mean of the temperatures measured by 6 T-type thermocouples,

$$\mathrm{T}_{w,o} = \frac{\sum_{i=1}^{6}(T_{w.o,i})}{6} \tag{4}$$

The local vapour quality is calculated using the following standard equations.

$$Hv = H_f + H_{fg} \tag{5}$$

where H_V is the total enthalpy in kJ/kg, H_f and H_{fg} are the enthalpies of liquid and enthalpy of the liquid-gas mixture in kJ/kg respectively.

$$x_{in} = (H_{in} - H_{f,in})/H_{fg,in} \tag{6}$$

where x_{in} is the inlet vapour quality of the test section, H_{in} is the enthalpy of the refrigerant at the inlet of the test section, in $\mathrm{kJ(kg)^{-1}}$, $H_{f,in}$ and $H_{fg,in}$ are the inlet enthalpies of liquid and liquid gas mixture corresponding to inlet pressure of the test section, in kJ/kg

$$H_{in} = H_{pre,in} + Q_{pre}/M \tag{7}$$

where,

H_{in} is the enthalpy of refrigerant at inlet of the test section in kJ/kg, Q_{pre} is the heat added to the preheater in W, $h_{pre,\,in}$ is the enthalpy corresponds to temperature and pressure at the inlet of the pre-heater section and *M* is the mass flow rate of the refrigerant in kg/s. The inlet enthalpy of the preheater is determined with the help of inlet temperature and pressure of the preheater (by using NIST refrigerant properties [28]).

$$x_{out} = (H_{out} - H_{f,out})/H_{fg,out} \tag{8}$$

where x_{out} is the outlet vapour quality of test section, h_{out} is the enthalpy at the outlet of the test section, kJ/kg, $H_{f,out}$ and $H_{fg,out}$ are the outlet enthalpies of liquid and liquid gas mixture respectively corresponding to the outlet pressure of the test section in kJ/kg.

The outlet enthalpy of the test section is determined by,

$$H_{\mathrm{out}} = H_{pre,in} + \frac{(Q_{pre} + Q_{test})}{\mathrm{M}} \tag{9}$$

where Q_{test} is the heat supplied at the test section in *W*.

The average vapour quality of the test section is the arithmetical mean of the inlet and the outlet vapour qualities.

$$x_{test} = \frac{x_{in} + x_{out}}{2} \tag{10}$$

where x_{test} is the average vapour quality in the test section.

2.5.2. Enhancement factor (EF)

In order to express the effect of the addition of nanoparticles to the refrigerant quantitatively, a term is introduced as enhancement factor (EF) [15] which is defined as the ratio between the heat transfer coefficients of refrigerant/nanolubricant mixture and the pure refrigerant/ lubricant mixture.

$$EF = \frac{h_{r,n,o}}{h_{r,o}} \tag{11}$$

$$EF\% = \left(\frac{h_{r,n,o} - h_{r,o}}{h_{r,o}}\right) * 100 \tag{12}$$

where $h_{r,n,o}$ and $h_{r,o}$ are the heat transfer coefficients of refrigerant nano-oil mixture (R134a/PAG/SiO_2) and refrigerant pure oil mixtures (R134a/PAG oil) respectively. If the value of EF is greater than 1, there is an upsurge in the heat transfer coefficient, whereas as if the value is less than 1 there is degradation in heat transfer coefficient and if the value of EF = 1, which indicates that nanoparticles have no influence on the heat transfer coefficient.

2.6. Validation of the experimental system with pure refrigerant

Before conducting experiments with nanolubricants, the experimental system is validated by conducting experiments with pure R134a refrigerant. The accuracy and reliability of the experimental test rig are evaluated by comparing the experimental data with that obtained from the model proposed by Panek et al. [20]. Regarding the slight differences in apparatus and operating conditions, trivial deviations are expected. The correlation proposed by Panek et al. is described here.

$$\frac{h_{tp}}{h_l} = \frac{3.686}{X^{0.563}} \tag{13}$$

where h_l is the heat transfer coefficient of the liquid phase h_{tp} is the two-phase heat transfer coefficient, *X* is the Lockhart-Martinelli parameter.

$$X = \left(\frac{1-x}{x}\right)^{0.9}\left(\frac{\rho_g}{\rho_l}\right)^{0.5}\left(\frac{\mu_l}{\mu_g}\right)^{0.1} \tag{14}$$

where *x* is the vapour quality, ρ_g *and* ρ_l are the vapour phase and liquid phase densities respectively. μ_l *and* μ_g corresponds to the liquid phase and vapour phase dynamic viscosities respectively.

$$h_l = \frac{0.023 k_l}{2 r_i}\ \ Re_l^{0.8}\ \ Pr_l^{0.4} \tag{15}$$

where, k_l is the liquid phase thermal conductivity, r_i is the inside radius of the test section. Re_l and Pr_l are the liquid phase Reynolds number and Prandtl number respectively.

2.7. Experimental uncertainty analysis

As far as the experimental investigations on heat transfer phenomena are concerned, the major uncertainties are related to the measurements of various parameters like temperature, pressure, mass flux, heat flux, etc. The standard uncertainty is the positive square root of the estimated variance of the individual uncertainties. This can be combined to obtain the expanded uncertainty and which has been calculated based on the law of propagation [24] of uncertainty in the following way.

$$\omega_R = \left[\left(\frac{\partial R}{\partial x_1}\omega_1\right)^2 + \left(\frac{\partial R}{\partial x_2}\omega_2\right)^2 + \ldots + \left(\frac{\partial R}{\partial x_n}\omega_n\right)^2\right]^{1/2} \tag{16}$$

where, ω_R is the uncertainty in the calculated result, $\omega_1, \omega_2, \ldots \omega_n$ be the uncertainties in the independent variables and $x_1, x_2, \ldots x_n$ are the independent variables.

The estimated uncertainty associated with the experimental study is summarized in the Table 2. The trial experiments are replicated for each experimental condition, and the repeatability of experimental heat transfer coefficients are found to be within 4.5%.

Table 2
Experimental uncertainties.

Experimental parameters	Uncertainty
Temperature (°C)	±0.5
Length (mm)	±0.5
Diameter (mm)	±0.1
Current (A)	±0.01
Voltage (V)	±0.01
Pressure (kPa)	±1
Mass flux (kg/m^{2}s)	±1.75%
Heat transfer coefficient (W/m^{2}K)	±6.57%

2.8. Tribological characterization of nanolubricant

The energy efficiency and overall performance of the refrigeration and air-conditioning systems can be improved by reducing the energy consumption by the refrigerant compressor. Frictional power loss is vital in determining the energy efficiency of compressors. Trivial saving in power consumption may result in overall performance improvement. Studies show that nanomaterials have the potential to improve the tribological properties of lubricants. Hence it is imperative to unveil the friction reduction and anti-wear potential of PAG based nanolubricants before actual application in refrigerant compressors. The friction reduction and anti-wear characteristics of the base lubricant (PAG oil) and the lubricant modified with SiO_2 nanoparticles are studied with a four-ball tribo-tester. The relative wear preventive characteristics and friction coefficients of nanolubricants and base oil are determined according to ASTM D 4172–94 and D 5183–05 standards respectively. This standard covers the procedures to evaluate the anti-wear characteristics of fluid lubricants using four-ball wear testing machine. Three balls which are known as bottom balls, having 12.7 mm diameter each are clamped together and which is submerged in the lubricant to be evaluated. The fourth ball, having the same diameter referred to as the top ball is pressed with a force of 392 N into the cavity shaped by the three balls so as to obtain three, point contacts. The test is performed under a regulated temperature of 75 °C. The top ball is rotated with an rpm of 1200 and the tests last for 60 min. AISI standard chrome steel (E-52100) with grade 25 extra polish with Rockwell C hardness 64–66 is used as the ball material. Wear preventive characteristics of lubricants are compared by using the average size of the scar diameters worn on the three lower clamped balls. An optical microscope with an accuracy of 0.001 mm is deployed to measure the wear scar diameter of the three stationary balls with the tester.

3. Results and discussion

SiO_2-PAG nanolubricants are prepared at different particle concentrations (0.1, 0.4, 0.6 and 0.8vol %). The morphological and stability studies are executed to portray the dispersion characteristics of nanolubricants. Forced convective heat transfer characteristics of pure R134a, R134a + pure PAG oil and R134a/SiO_2nanorefrigerant (R134a + SiO_2-PAG nanolubricant) in a horizontal smooth tube has been carried out at different mass fluxes, heat fluxes, vapour qualities, and particle concentrations. Tribological studies are performed to explicate the friction reduction and anti-wear characteristics of nanolubricant.

3.1. Flow boiling heat transfer

Experiments are conducted with pure R134a, R134a + pure PAG lubricant (2% mass fraction) and R134a + SiO_2-PAG nanolubricant. The heat flux is varied from 0.45 to 5 kW/m and vapour quality from 0 to 0.5. Two different mass fluxes of 34 and 47 kg/m^2 s are considered. The particle concentrations selected for the study are 0.1, 0.4 and 0.8 vol%. For validating the experimental setup, experimental heat transfer coefficients for pure R134a are compared with those predicted from Panek et al. correlation [20]. The comparison between experimental data and that predicted from correlation is shown in Fig. 4.

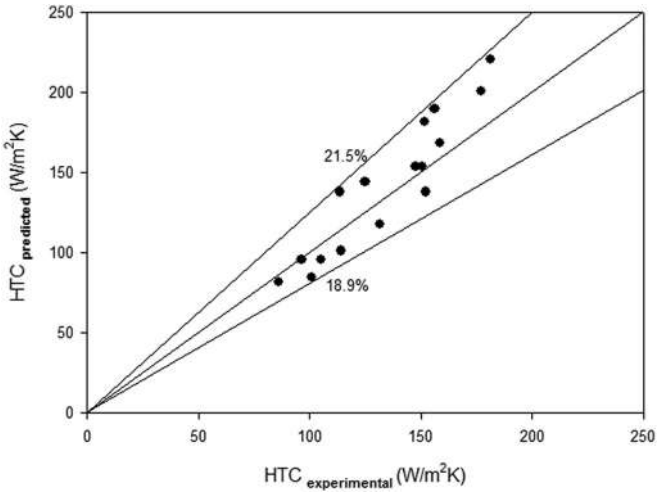

Fig. 4. Comparison of experimental data with correlation.

The deviation of experimental data with respect to correlation prediction is from 1.95% to 21.5%. The average deviation recorded is 11.35%. Most of the experimental values are well below that maximum noted deviation. The specified deviation may regard to the slight differences in apparatus and operating conditions. Deviation in a similar fashion is reported by Henderson et al. [10]. The good agreement of experimental values of heat transfer coefficient inspires to perform further experimentation with the same experimental test rig.

3.1.1. Flow boiling heat transfer of pure R134a and R134a/PAG oil

Hermetic compressors are widely used in vapour compression refrigeration systems, in which, oils are intrinsic to lubricate the sliding surfaces. During functioning, the refrigerant carries the traces of lubricant and reaches the evaporative section. The presence of oil becomes a key determinant on thermophysical properties of refrigerant such as surface tension, viscosity, and thermal conductivity. Besides, it may also become a vital factor in the formation of flow regime and eventually in the heat transfer characteristics of refrigerant in the evaporator.

In order to perceive the effect of lubricating oil on the heat transfer coefficient, experiments are conducted with pure refrigerant and refrigerant and PAG oil mixture. The experimental results of the heat transfer coefficient of pure R134a and R134a/PAG lubricant at different vapour qualities and mass fluxes are shown in Fig. 5

Pure R134a displays a higher heat transfer coefficient than that of R134a-PAG mixture, especially at lower vapour qualities, at the two tested mass fluxes. At higher vapour qualities, the refrigerant oil mixture marginally enhances the heat transfer coefficient, i.e. at higher vapour qualities, the presence of lubricating oil contribute to the slight upsurge in the HTC. Similar trends are reported for the case of HFC-134a/PAG oil mixture and CFC-12/mineral oil mixture [25]. The enhancement in heat transfer apparently depends on the heat flux, the flow rate, flow patterns, the type of tube, etc. As the vapour quality increases, the process of vaporization progresses and the concentration of oil becomes higher enough to cause phase separation, i.e. an oil-rich phase and refrigerant rich phase. The former may acts as a coating at the tube surface top and the latter flows through the lower portion of the horizontal tube. The refrigerant portion in the oil-rich phase still evaporates as the heat is conducted from the wall through the oil film and eventually the heat transfer coefficient increases. As the mass flux increases from 34 kg/m^2 s to 47 kg/m^2 s, the difference in HTC between the pure refrigerant and refrigerant oil mixture is found to be marginal. More specifically, at lower mass flux, the presence of oil decreases the average heat transfer coefficient of pure refrigerant by 24%.

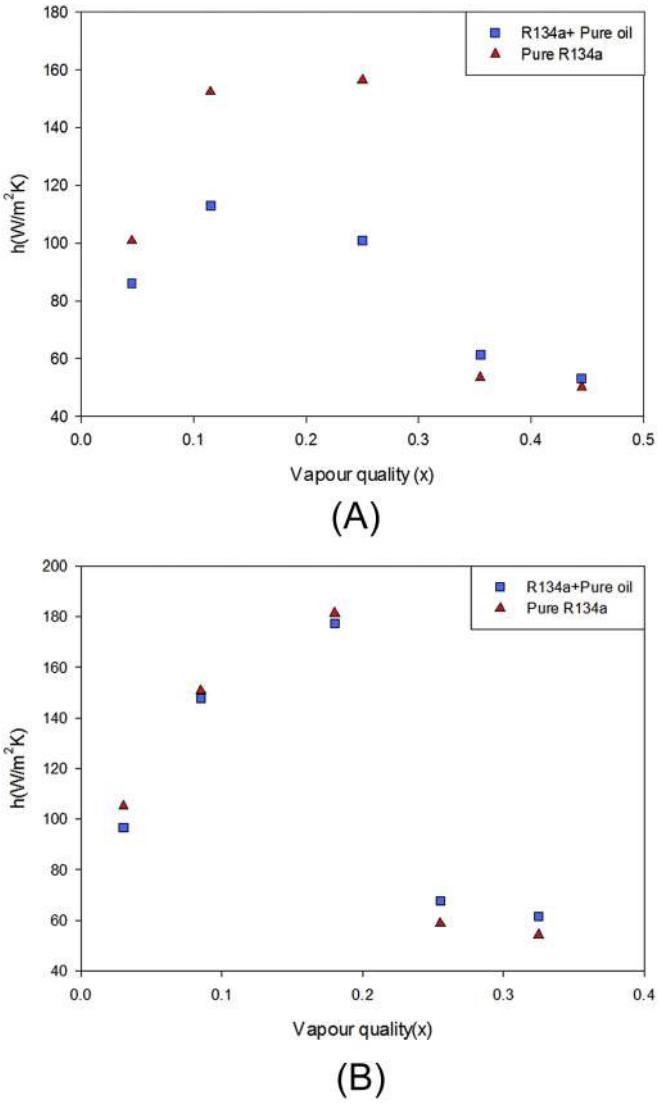

Fig. 5. Comparison of the flow boiling heat transfer coefficient of R134a/PAG oil and pure R134a (a) at mass flux 34 kg/m^2 s (b) at mass flux 47 kg/m^2 s.

Nonetheless, at higher mass flux, it is observed as 8.18%. The HTC found to be increased with an increase in mass flux. This reason for this is, by increasing the mass flow rate consequences increase in flow velocity and hence increase in Reynolds number, and transition of flow regime. At lower mass fluxes the flow regime may be in the stratified region, as mass velocity increases, the flow regime may transform into an annular pattern. Heat transfer coefficients are characteristically much higher in the annular regime than in the stratified regime. The mass fraction of lubricant is limited to 2% because mass fraction beyond 2% results in a significant deterioration in heat transfer [20].

3.1.2. Flow boiling heat transfer of R134a/PAG oil and R134a/SiO_2–PAG nano-oil

With an aim to identify the effect of nanoparticles on the heat transfer coefficient of refrigerant, experiments are conducted with refrigerant/pure lubricant mixture and refrigerant/ nanolubricant mixture with different volume fractions under identical test conditions. Mass flux is varied to expose the impact of mass flux on HTC.

Fig. 6 shows the comparison of the heat transfer coefficient of refrigerant/pure lubricant and refrigerant/nanolubricant at various volume fractions and mass fluxes. It is obvious from the figures that the presence of nanoparticles in the refrigerant has a crucial impact on the flow boiling heat transfer characteristics. It is evident from the figure that the presence of nanoparticles in the refrigerant manifested higher heat transfer coefficient than that of refrigerant/pure lubricant mixture at all the mass fluxes considered. From the figures, it is also clear that as the mass flux increases, the heat transfer coefficient also increases. The increase in HTC is due to higher liquid velocities at higher mass flux and transformation of flow regimes. Nanolubricant with particle concentrations 0.1, 0.4 and 0.8 vol% exhibits enhanced heat transfer coefficients at all experimental conditions than the baseline tests with pure lubricant. But for the case of 0.8% volume fraction, the heat transfer coefficient diminishes at higher vapour qualities. At higher particle concentration (0.8vol %), it is conjectured that the viscosity of nanorefrigerant plays a key role in HTC. The maximum heat transfer coefficient is exhibited by the nanolubricant refrigerant mixture at a particle concentration of 0.4 vol%. The maximum value of HTC observed for nanolubricants at 0.1, 0.4 and 0.8 vol% are 174.22, 232.57 and 177.68 W/m^2 K respectively at a mass flux of 34 kg/m^2 s and the corresponding heat transfer coefficient for a mass flux of 47 kg/m^2 s is 196.12, 219.31 and 190 W/m^2 K respectively. Among the volume fractions considered, nanolubricant at a volume fraction of 0.4% exhibits a maximum increase in heat transfer coefficient by 31% and 34% compared to 0.8 and 0.1 vol% nanolubricants respectively.

As the vapour quality increases, the local oil concentration in the two-phase fluid turns out to be greater because lubricating oils have a

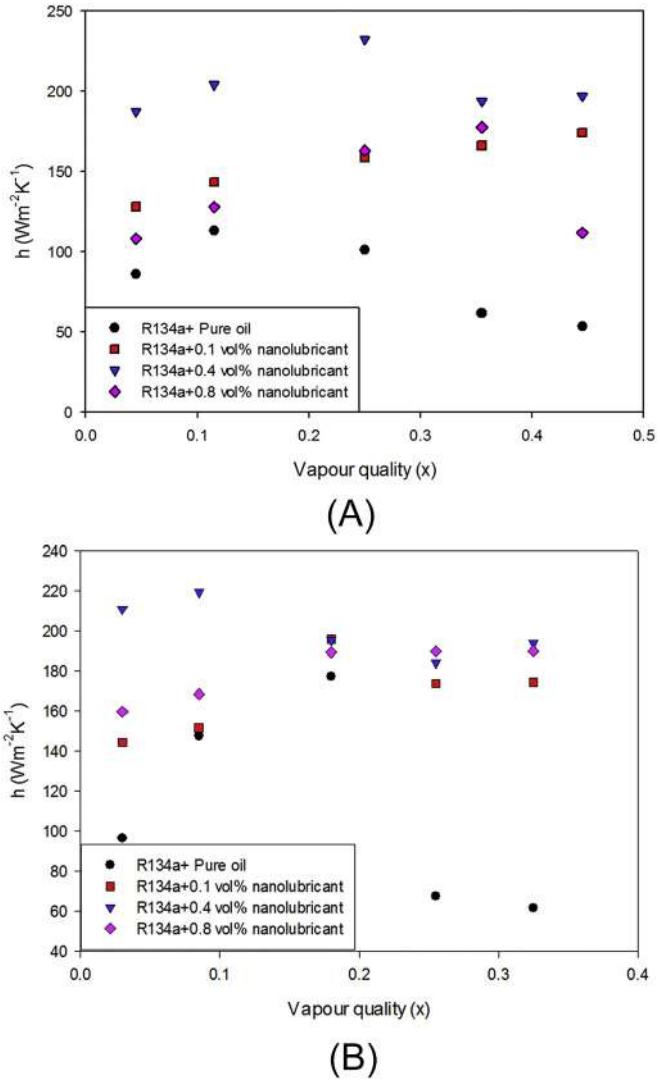

Fig. 6. Heat transfer coefficient versus vapour quality at (a) mass flux of 34 kg/m^2 s (b) mass flux of 47 kg/m^2 s.

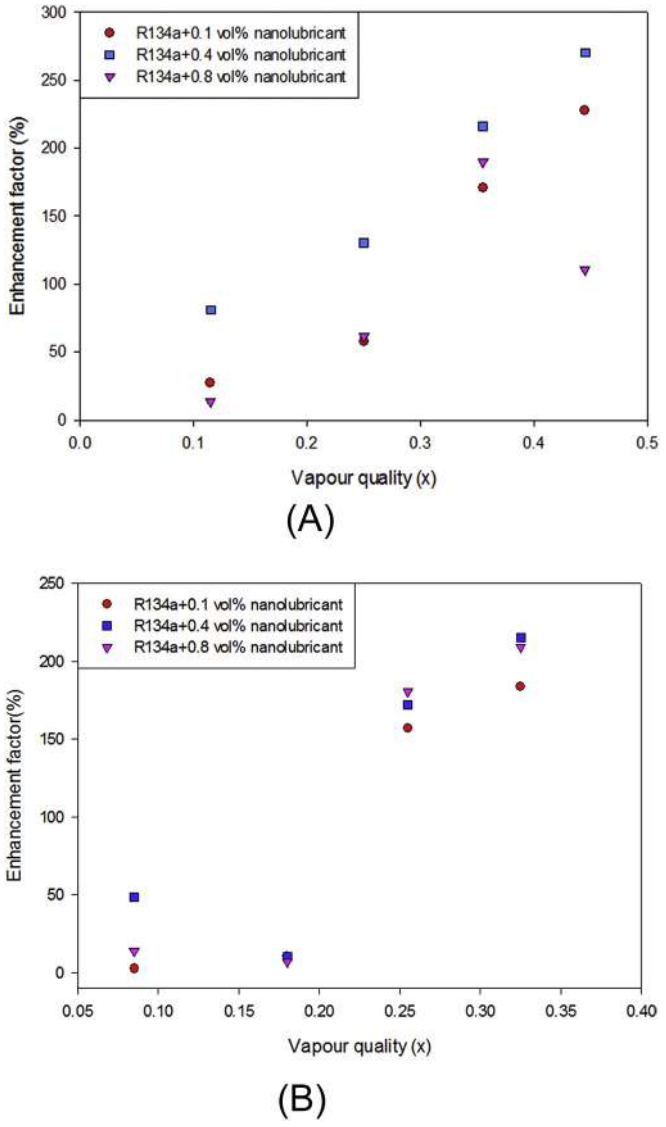

Fig. 7. EF versus vapour quality at (a) mass flux 34 kg/m^2 s (b) mass flux 47 kg/m^2 s.

higher boiling point than that of refrigerant. Higher dosing level of particles may result in augmented viscosity of lubricant, which in turn penalties the Reynolds number. Due to this, the heat transfer enhancement caused by turbulent mixing and agitation between bubbles and nanoparticles may be suppressed and which leads to a detrimental effect in the HTC at elevated particle concentrations. Even though the nanolubricant at higher volume fraction (0.8 vol%) manifested a decrease in HTC, it is on the higher side than that of pure lubricant at all the tested conditions.

At all particle concentrations, nanolubricant displays enhanced heat transfer performance than that of refrigerant/pure lubricant mixture.

The dominant mechanisms of this dramatic improvement in heat transfer characteristics are: (i) The presence of nanoparticles in the base fluid increases the thermal conductivity of the fluid [29] (ii) It is conjectured that the active nanoparticles interact with the bubbles and collapses in a quicker fashion. This phenomenon causes more liquid to come in contact with the heated surface and which leads to a decrease in wall superheat required to initiate nucleation of bubbles. Moreover, the active nucleation site density may also enhance due to the presence of nanoparticles [30,31] (iii) the nanoparticles may form a porous layer on the surface and increases the number of nucleation sites. Furthermore, nano-sized particles can infiltrate into the bubble zone near the heated wall surface and comes in contact with the surface of the thermal boundary layer so as to generate more bubbles instantly [32] (iv) There may be dynamic changes in the surface roughness of the flow conduits due to intermittent activation and suppression of nucleation sites and which in turn to be the major contributing factor for increased nucleation boiling and heat transfer coefficients.

The effect of the addition of nanoparticle to the base refrigerant is quantitatively measured by the enhancement factor. Fig. 7 shows the EF (enhancement factor) for nanorefrigerants at 0.1, 0.4 and 0.8% volume fraction at two different mass fluxes. The enhancement factor increases with an increase in particle concentration. However, for the case of 0.8 vol% particle concentration, there is a decline in EF is noticed at moderate vapour qualities. This can be explained as when the vapour quality increases, the refrigerant content in the two-phase mixture decreases and the fluid will be rich in the lubricant. At increased particle concentrations, the presence of nanoparticles in the lubricant will be higher and the viscosity may also be at the higher side and this viscous effect eventually decreases heat transfer coefficient. The maximum enhancement was manifested by R134a-SiO_2 nanolubricant at 0.4% volume fraction. The average increase in heat transfer enhancement factor for 0.1, 0.4, and 0.8 vol% are 106.3%, 163.16% and 80.4% respectively.

Fig. 8 provides an ample conclusion of the heat transfer enhancing potential of nanoparticles at a glance. It is evident from the figure that, the heat transfer coefficient of refrigerant nanolubricant mixture is higher than that of pure refrigerant regardless of the mass fluxes and heat fluxes considered. The factors which supplement for the enhanced heat transfer phenomena other than the dominant factors mentioned in the previous section are (i) the particle surface adhesion property, different types of the particle should have different surface adhesion property. (ii) As the nanoparticle concentration increases, the interaction between the particles also increases and which leads to an increase in heat transfer performance. (iii) the presence of nanoparticles enhances the thermal conductivity of the refrigerant. (iv) the increased surface tension of nanorefrigerant at lower vapour qualities may results in increased wettability than the pure refrigerant (v) the presence of nanoparticles disturbs the boundary layer formation and eventually decreases the boundary layer thickness, which reduces the thermal resistance and leads to enhanced heat transfer [12].

3.2. Pressure drop characteristics

The general trend of pressure drop observed for both R134-pure lubricant and R134a-nanolubricant is that, as the vapour quality increases, pressure drop also increases. At lower concentrations (0.1 and 0.4 vol%),

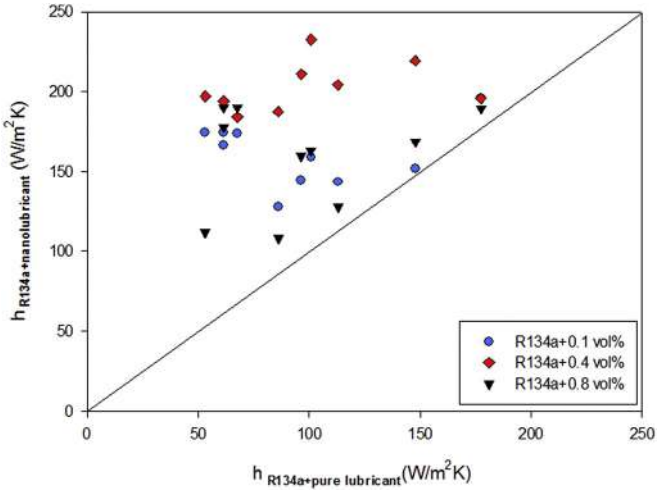

Fig. 8. Comparison of heat transfer coefficient between R134/nanolubricant and R134a/pure lubricant.

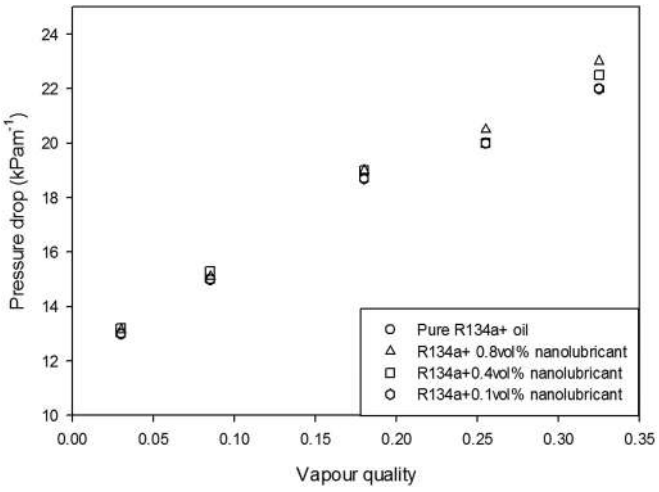

Fig. 9. Comparison of pressure drop between R134a/oil and R134a/nanolubricant at a mass flux of 47 kg/m^2 s.

refrigerant/nanolubricant mixture exhibits insignificant variation in pressure drop compared to pure refrigerant/lubricant mixture, within the experimental uncertainty. However, a slight increase in pressure drop is displayed by nanolubricant at a particle dosing level of 0.8 vol% particularly at higher vapour qualities. The possible reason is that as the vapour quality increases the flow transforms into shear dominant and consequently turbulence is generated by high-velocity vapour, which generates more friction against the liquid phase. As the particle volume fraction increases, the phenomenon becomes more prominent. Moreover, the increase in the population of nanoparticle enhances the wall interaction and augments the collision between the particles. The maximum increase in pressure drop measured is 4.5% compared to pure refrigerant lubricant mixture. However, the recorded penalty in pressure drop is insignificant compared to the enhanced heat transfer capability, which in turn benefices the overall energy efficiency. The variation in pressure drop is portrayed in Fig. 9. A similar trend, i.e., insignificant pressure drop penalty was reported in the literature by Bartelt et al. [26] for in-tube flow boiling of refrigerant/CuO nanolubricant.

3.3. Tribological studies

The friction reduction and anti-wear characteristics of the base PAG lubricant and the lubricant modified with SiO_2 nanoparticles with different volume fractions (0.1, 0.4 and 0.6 vol%) are determined with a four-ball tribo-tester according to ASTM D 5183–05 and D 4172–94 standards.

3.3.1. Frictional torque and friction coefficient

The time-dependent frictional torque and friction coefficient for pure lubricant and nanolubricants at different particle concentrations are evaluated. The wear preventive potential of nanolubricant has been evaluated by examining the wear scar morphology. The friction reduction characteristics of SiO2-PAG nanolubricants is portrayed in Fig. 10.

From figures, it is evident that SiO_2 nanoparticles have a significant role in the friction reduction capability of PAG lubricant. A substantial diminution in the frictional torque and coefficient of friction is noticed at all volume fractions considered, with respect to pure PAG lubricant. The coefficient of friction is reduced by 1.02%, 28.57% and 37.76% for 0.1, 0.4 and 0.6 vol% respectively. For the case of SiO_2 nanolubricant, it is also observed that as the particle concentration increases, the friction reduction capability also increases. The coefficient of friction is found to be slightly increased at the beginning of the test and as the time elapses it gets stabilized. This is due to the initial polishing effect.

The mechanisms that are responsible for the wear prevention characteristics of nanolubricants are categorized into two. The direct effect of nano-additives, viz. the ball bearing effect and surface protective tribo-film formation and the secondary mechanisms viz. mending or repairing effect, polishing and smoothing effect [19]. The ball bearing effect is prominent in the case of spherical or quasi-spherical nanoparticles. The nanoparticles dispersed in the lubricants are supposed to act as minute ball bearings between the contact regions. The sliding contact configuration between the counterparts is thus transformed to pure rolling configuration or a mixture of rolling and sliding nature.

The formation of tribo-film between the interacting surfaces is due to the reaction between the nano-additives and surfaces under the operating and environmental conditions. The tribo-film formation is governed by nature and type of the nanoparticles and the interacting surfaces. Due to the interlocking of surface asperity and subsequent welding and detachment, there may be loss in mass of the sliding surfaces. The secondary effect such as mending or self-repairing effect comes in the picture at this moment. The nanoparticles compensate for the loss of material by depositing at the wear scars and grooves and which diminishes the abrasive wear. The nanomaterials exhibit entirely different mechanical, thermal and electrical properties than its bulk material

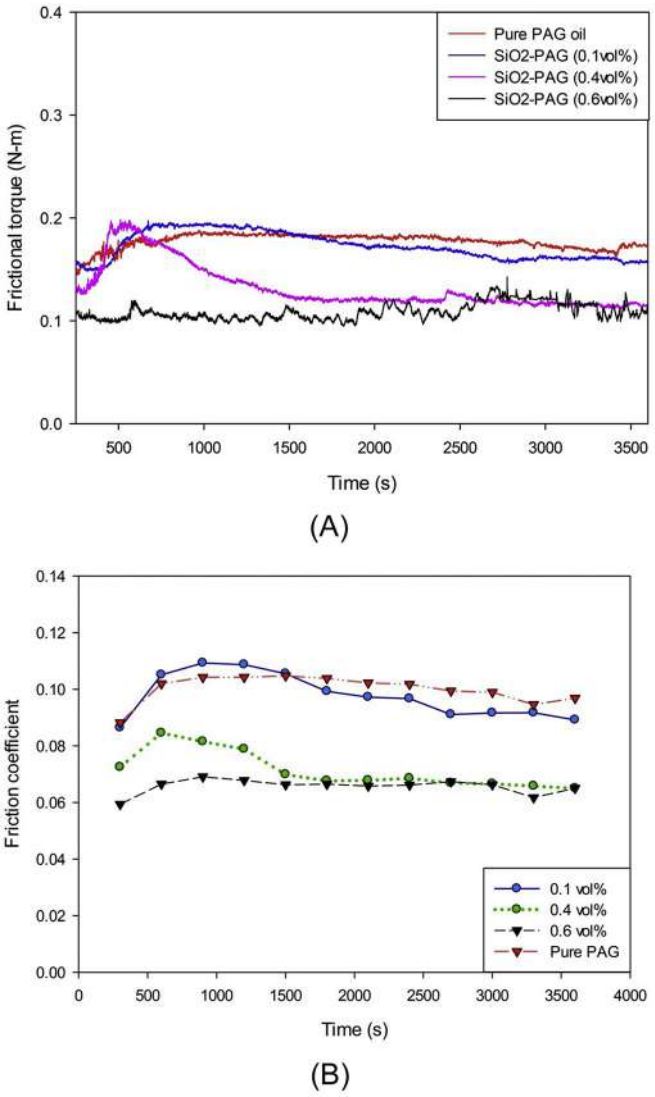

Fig. 10. Comparison of (a) frictional torque of SiO_2-PAG nanolubricant (b) friction coefficient of SiO_2-PAG nanolubricant with pure lubricant.

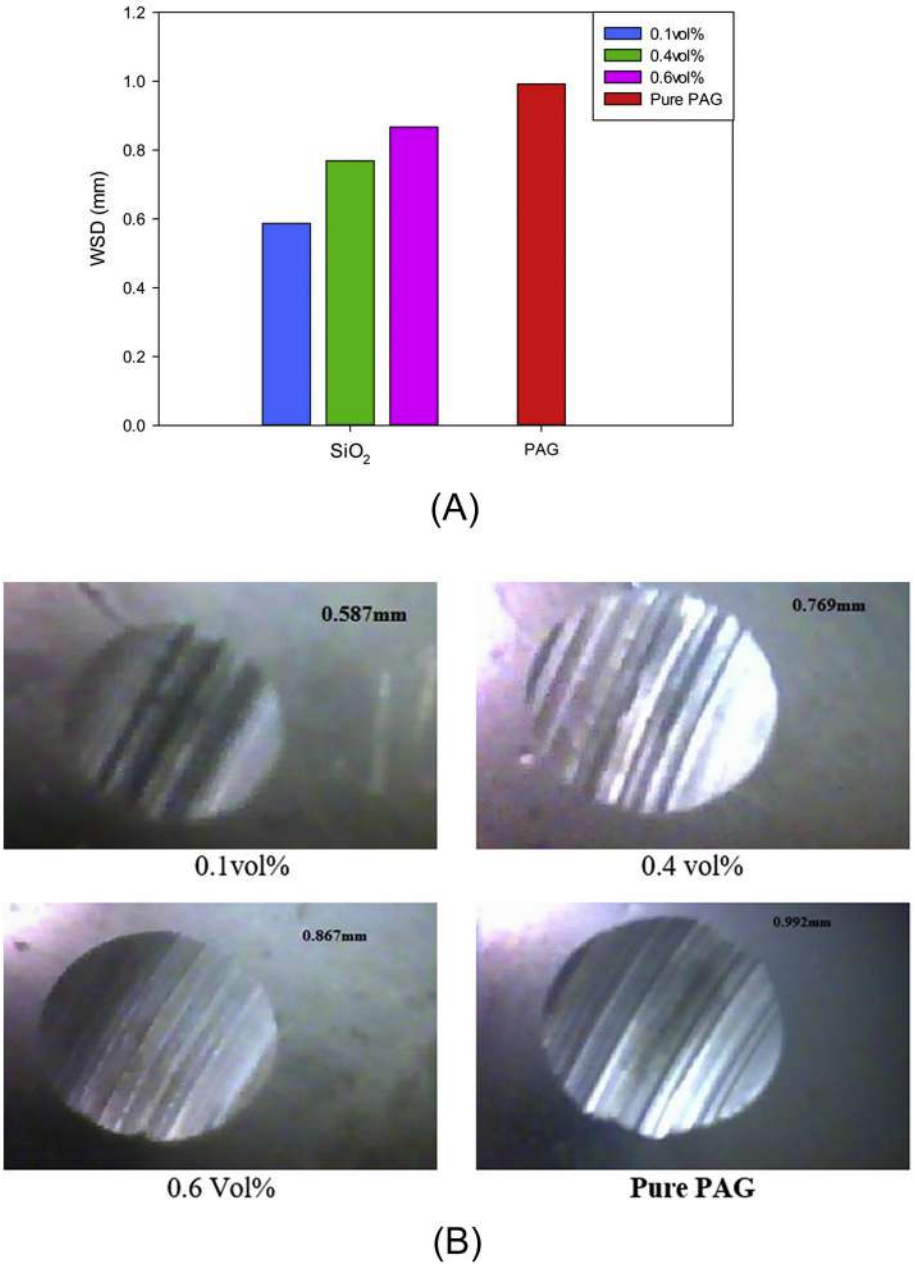

Fig. 11. Comparison of (a) Wear scar diameters (b) Wear scar images.

when they are downscaled to nano-size. According to the Hall-Petch strengthening effect, the mechanical properties like hardness and yield strength of nanoparticles increase with a reduction in particle size [27]. The polishing effect is attributed by the nanoparticle aided abrasion. The surface asperities could be eliminated by three-body abrasion. Thus roughness of the contact surfaces gets reduced and it gets polished. This will lead to a reduction in the friction coefficient. Besides, during the smoothing process, the space between the surface asperities may act as the sump of nanoparticles and the particles may fill the gaps which in turn diminish the interlocking of surface asperities. The aforementioned multiple mechanisms contribute to the enhanced tribological characteristics with nanolubricants.

3.3.2. Wear preventive property of SiO2-PAG nanolubricant

The anti-wear characteristics of lubricants can be evaluated from the wear scar morphology, especially from the wear scar diameter. The load-carrying capacity and degree of wear depend on the wear scar diameter (WSD). Greater the wear scar diameter, greater will be the wear rate and lesser will be the load-bearing capacity of the lubricating oil and vice-versa. The wear scar diameter of the bottom balls is measured using an optical microscope.

From Fig. 11 (a) and (b) it can be concluded that the SiO_2-PAG nanolubricant at all volume concentrations demonstrated good anti-wear property compared to the pure lubricant. The reduction in wear scar diameter is maximized at 0.1 vol% by 40.83%. The corresponding reduction in wear scar diameter for particles concentrations 0.4 and 0.6 vol% are 22.48% and 12.6% respectively.

The increase in particle concentration increases the wear scar diameter and thus reduces the relative wear preventive characteristics. This is due to the abrasive nature of the agglomerated particles under severely loaded conditions. Moreover, at higher nanoparticle concentrations, the spherical shape of the nanoparticle will be altered. This will eventually modify the nature of contact from rolling to

sliding configuration. Furthermore, if the nanoparticle cluster size is higher than the space between the surface asperities in the mating parts, it could not penetrate between the surface asperities. The nano racemes will be then accumulated around the contact zone and which in turn serves as a barrier and hiders the free flow of lubricant into the region. These effects enhance the wear rate and reduce the wear prevention characteristics [19]. However, a substantial reduction in wear scar diameter is manifested by SiO_2-PAG nanolubricant compared to the pure lubricant at all the particle concentrations considered in the present investigation. Among the particle concentration considered, nanolubricant at 0.4 vol% can be an effective option in the friction reduction and anti-wear perspective. The prominent mechanisms for the better anti-wear characteristics of nanolubricants are attributed to the increased probability of penetration of the nanoparticles and their anchoring at the interfaces, which prevents the metal-to-metal contact and the presence of a strong and durable tribo-film [36].

4. Conclusions

The heat transfer characteristics of R134a refrigerant appended with SiO_2-PAG nanolubricant and anti-wear potential of SiO_2-PAG nanolubricant are experimentally evaluated. The energy efficiency of refrigeration systems primarily depends on the heat transfer capability of the working fluid. Trivial savings in power consumption in compressors are also found to contribute to the overall system performance enhancement. The following conclusions are derived out of this study (i) the heat transfer coefficient increases with increase in mass flux for both refrigerant/lubricant mixture and refrigerant/nanolubricant mixtures (ii) R134a/SiO_2 nanolubricant exhibits significant improvement in the flow boiling heat transfer coefficient than pure refrigerant at all particle concentrations considered (iii) the maximum flow boiling heat transfer coefficient is observed at a volume fraction of 0.4%, and at this volume fraction, the average enhancement factor is observed as 163.2%. (iv) the nanorefrigerant displays marginal increase in pressure drop compared to R134-pure-PAG mixture (v) SiO_2-PAG nanolubricant exhibits superior friction reduction and anti-wear capability than pure lubricant (vi) at volume fractions of 0.6 and 0.4%, significant reduction in coefficient of friction is manifested (37.76 and 28.57% respectively) (vii) the wear scar diameter is decreased by 40.83% and 22.48% at 0.1 and 0.4 vol% respectively (viii) considering the heat transfer and tribological characteristics, the optimum particle concentration is found to be 0.4 vol% (ix) addition of nanoparticles improves the overall performance of refrigeration systems and which may lead to the development of energy-efficient and compact HVAC systems.

References

[1] M.L. Levin, M.A. Miller, Maxwell's, Treatise on Electricity and Magnetism, 2nd ed.vol. 135, Clarendon Press, 1981 425.

[2] J.A. Eastman, S.U.S. Choi, S. Li, L.J. Thompson, S. Lee, Enhanced thermal conductivity through the development of nanofluids, MRS Proc. 457 (1997) 3–11, https://doi.org/10.1557/PROC-457-3.

[3] V. Nair, P.R. Tailor, A.D. Parekh, Nanorefrigerants:- a comprehensive review on its past, present and future, Int. J. Refrig. 67 (2016) 290–307, https://doi.org/10.1016/j.ijrefrig.2016.01.011.

[4] N. Subramani, M.J. Prakash, Experimental studies on a vapour compression system using nanorefrigerants, Int. J. Eng. Sci. Technol. 3 (2011) 95–102.

[5] A. Sozen, E. OZbas, T. Menlik, M.T. Cakir, M. Guru, K. Boran, Improving the thermal performance of diffusion absorption refrigeration system with alumina nanofluids: an experimental study, Int. J. Refrig. 44 (2014) 73–80, https://doi.org/10.1016/j.ijrefrig.2014.04.018.

[6] M.Z. Sharif, W.H. Azmi, A.A.M. Redhwan, R. Mamat, T.M. Yusof, Performance analysis of SiO2/PAG nanolubricant in automotive air conditioning system, Int. J. Refrig. (2017)https://doi.org/10.1016/j.ijrefrig.2017.01.004.

[7] D.W. Liu, C.-Y. Yang, Effect of Nano-Particles on Pool Boiling Heat Transfer of Refrigerant 141b, Icnmm200730221 2007 789–793, https://doi.org/10.1115/ICNMM2007-30221.

[8] K.J. Park, D. Jung, Enhancement of nucleate boiling heat transfer using carbon nanotubes, Int. J. Heat Mass Transf. 50 (2007) 4499–4502, https://doi.org/10.1016/j.ijheatmasstransfer.2007.03.012.

[9] H. Peng, G. Ding, H. Hu, W. Jiang, D. Zhuang, K. Wang, Nucleate pool boiling heat transfer characteristics of refrigerant/oil mixture with diamond nanoparticles, Int. J. Refrig. 33 (2010) 347–358, https://doi.org/10.1016/j.ijrefrig.2009.11.007.

[10] K. Henderson, Y. Park, L. Liu, A.M. Jacobi, International journal of heat and mass transfer flow-boiling heat transfer of R-134a-based nanofluids in a horizontal tube, Int. J. Heat Mass Transf. 53 (2010) 944–951, https://doi.org/10.1016/j.ijheatmasstransfer.2009.11.026.

[11] B. Sun, D. Yang, Flow boiling heat transfer characteristics of nano-refrigerants in a horizontal tube, Int. J. Refrig. (2013), https://doi.org/10.1016/j.ijrefrig.2013.08.020.

[12] M.A. Akhavan-Behabadi, M. Nasr, S. Baqeri, Experimental investigation of flow boiling heat transfer of R-600a/oil/CuO in a plain horizontal tube, Exp. Thermal Fluid Sci. 58 (2014) 105–111, https://doi.org/10.1016/j.expthermflusci.2014.06.013.

[13] S. Bobbo, L. Fedele, M. Fabrizio, S. Barison, S. Battiston, C. Pagura, Influence of nanoparticles dispersion in POE oils on lubricity and R134a solubility, Int. J. Refrig. 33 (2010) 1180–1186, https://doi.org/10.1016/j.ijrefrig.2010.04.009.

[14] M. Kole, T.K. Dey, Thermophysical and pool boiling characteristics of ZnO-ethylene glycol nanofluids, Int. J. Therm. Sci. 62 (2012) 61–70, https://doi.org/10.1016/j.ijthermalsci.2012.02.002.

[15] M.A. Akhavan-Behabadi, F. Hekmatipour, S.M. Mirhabibi, B. Sajadi, Experimental investigation of thermal-rheological properties and heat transfer behavior of the heat transfer oil-copper oxide (HTO-CuO) nanofluid in smooth tubes, Exp. Thermal Fluid Sci. 68 (2015) 681–688, https://doi.org/10.1016/j.expthermflusci.2015.07.008.

[16] M. Hemmat Esfe, S. Saedodin, An experimental investigation and new correlation of viscosity of ZnO-EG nanofluid at various temperatures and different solid volume fractions, Exp. Thermal Fluid Sci. 55 (2014), https://doi.org/10.1016/j.expthermflusci.2014.02.011.

[17] N. Rajendhran, S. Palanisamy, P. Periyasamy, R. Venkatachalam, Enhancing of the tribological characteristics of the lubricant oils using Ni-promoted MoS2nanosheets as nano-additives, Tribol. Int. 118 (2018) 314–328, https://doi.org/10.1016/j.triboint.2017.10.001.

[18] Castillo and Spikes (2000), F. Chinas-Castillo, H.A. Spikes, The behavior of colloidal solid particles in elasto hydrodynamic contacts, Tribol. Trans. 43 (3) (2000) 387–394.

[19] M. Gulzar, H.H. Masjuki, M.A. Kalam, M. Varman, N.W.M. Zulkifli, R.A. Mufti, R. Zahid, Tribological performance of nanoparticles as lubricating oil additives, J. Nanopart. Res. 18 (8) (2016) 223.

[20] J.S. Panek, J.C. Chato, J.M.S. Jabardo, A.L. Souza, J.P. De Wattelet, Evaporation Heat Transfer and Pressure Drop in Ozone-Safe Refrigerants and Refrigerant-Oil Mixtures, 1992 61801.

[21] J.R. Thome, Comprehensive thermodynamic approach to modeling refrigerant-lubricating oil mixtures, HVAC&R Res. 1 (1995) 110–125, https://doi.org/10.1080/10789669.1995.10391313.

[22] Y.Takaishi, K.Oguchi, Measurements of vapor pressure of R-22/oil solutions, Proceedings of the 18th International Congress of Refrigeration, Vienna 1987, pp. 217–222.

[23] E.P. Bandarra Filho, L. Cheng, J.R. Thome, Flow boiling characteristics and flow pattern visualization of refrigerant/lubricant oil mixtures, Int. J. Refrig. 32 (2009) 185–202, https://doi.org/10.1016/j.ijrefrig.2008.06.013.

[24] J.P. Holman Holman, W.J. Gajda, Experimental Methods for Engineers, McGraw-Hill, New York, 2001.

[25] T. Fukushima, M. Kudou, Heat transfer coefficients and pressure drop for forced convection boiling and condensation of HFC 134a, Proceedings, ASHRAE-Purdue CFC Conference 1990, pp. 196–204.

[26] K. Bartelt, Y. Park, A. Jacobi, Flow-Boiling of R-134a/POE/CuO Nanofluids in a Horizontal Tube, International Refrigeration and Air Conditioning Conference, Paper 928, http://docs.lib.purdue.edu/iracc/928 2008.

[27] W. Xu, L.P. Dávila, Tensile nanomechanics and the hall-Petch effect in nanocrystalline aluminium, Mater. Sci. Eng. A 710 (2018) 413–418, https://doi.org/10.1016/j.msea.2017.10.021.

[28] NIST Standard Reference Data Program, REFPROP v9.1, Reference Fluid Thermodynamic andTransport Properties, 2013 (Boulder, CO).

[29] S.S. Sanukrishna, S. Vishnu, M. Jose Prakash, Experimental investigation on thermal and rheological behaviour of PAG lubricant modified with SiO 2 nanoparticles, J. Mol. Liq. 261 (2018) 411–422.

[30] Gobinath and Venugopal 2019, N. Gobinath, T. Venugopal, Nucleate pool boiling heat transfer characteristics of R600a with CuO nanoparticles, J. Mech. Sci. Technol. 33 (2019) 465–473, https://doi.org/10.1007/s12206-018-1246-x.

[31] H. Peng, G. Ding, H. Hu, W. Jiang, D. Zhuang, K. Wang, Nucleate pool boiling heat transfer characteristics of refrigerant/oil mixture with diamond nanoparticles, Int. J. Refrig. 33 (2010) 347–358, https://doi.org/10.1016/j.ijrefrig.2009.11.007.

[32] K.J. Park, D. Jung, Enhancement of nucleate boiling heat transfer using carbon nanotubes, Int. J. Heat Mass Transf. 50 (2007) 4499–4502, https://doi.org/10.1016/j.ijheatmasstransfer.2007.03.012.

[33] L. Yang, J. Xu, K. Du, X. Zhang, Recent developments on viscosity and thermal conductivity of nanofluids, Powder Technol. 317 (2017) 348–369.

[34] N.N. Esfahani, D. Toghraie, M. Afrand, A new correlation for predicting the thermal conductivity of ZnO–Ag (50%–50%)/water hybrid nanofluid: an experimental study, Powder Technol. 323 (2018) 367–373.

[35] S.K. Das, S.U.S. Choi, Nanofluids Science and Technology, A John Wiley & Sonc. Inc., Publication, New Jersey, Canada, 2007.

[36] A. Verma, W. Jiang, H.H. Abu Safe, W.D. Brown, A.P. Malshe, Tribological behavior of deagglomerated active inorganic nanoparticles for advanced lubrication, Tribol. Trans. 51 (2008) 673–678, https://doi.org/10.1080/10402000801947691.